Transferred-Substrate InP-Based Heterostructure Barrier Varactor Diodes on Quartz

S. Arscott, T. David, X. Mélique, P. Mounaix, O. Vanbésien, and D. Lippens

***Abstract*—InP-based heterostructure barrier varactor (HBV) devices employing air-bridge technology have been fabricated on a quartz host substrate following a transfer-substrate technique. Electrical characterization demonstrates highly symmetrical $I(V)$ and $C(V)$ characteristics due to the preservation of the high quality MBE epitaxial layers during the transfer process. Small signal RF measurements have been performed up to 110 GHz and display a marked reduction in the values of parasitic resistance and capacitance, thus confirming the ability of the devices to operate in the upper-part of the mm spectrum.**

***Index Terms*—Heterojunction barrier varactor diode, InP-based materials, substrate-transfer, Terahertz frequency.**

I. Introduction

IN ORDER to develop III–V based microwave devices which operate in the upper part of the millimeter and submillimeter wave spectrum, i.e., the Terahertz gap, substrate-transfer and membrane-like techniques are now widely being developed [1]–[4]. Such techniques have several advantages, e.g., low dispersion to wave propagation, low thermal integration, substrate-mode suppression and a reduction in the values of the extrinsic parasitic elements.

A potential component for frequency tripling and quintupling in the Terahertz gap is the heterostructure barrier varactor (HBV) diode [5]. InP-based HBV devices fabricated by the authors have shown record performances in terms of efficiency (12.3%) and output power (9 mW) at a frequency of 250 GHz [6], [7]. Following these results, we proposed a new transfer-substrate technique enabling us to fabricate InP-based HBV diodes on glass substrate [4], [8].

In this letter, we extend these ideas in order to fabricate transferred-substrate air-bridge connected HBV devices on 70 μm thick quartz substrate. We also demonstrate the usefulness of the epitaxial liftoff (ELO) and transfer-substrate techniques toward dramatically reducing the parasitic elements of such devices.

II. Device Fabrication

The dual barrier HBV epitaxial layers were fabricated in a *Riber* gas-source MBE system using InP-based technology. A dual barrier scheme is used, composing of two $In_{0.52}Al_{0.48}As$ (50 Å)/AlAs (50 Å)/$In_{0.52}Al_{0.48}As$ (50 Å) barriers lying between $In_{0.53}Ga_{0.47}As$ (3000 Å) cladding layers doped to $N_d = 2 \times 10^{17}$ cm^{-3}. The thickness of AlAs barriers has been increased from 30 Å to 50 Å for this study in order to further reduce the leakage current. It should be noted that the narrow gap of the InGaAs cladding layers is an advantageous feature for very high frequency operation, notably by alleviating saturation current effects at moderate doping levels. In addition, the doping density of the $n^+In_{0.53}Ga_{0.47}As$ ohmic contact layers has been increased from $N_d = 5 \times 10^{18}$ cm^{-3}, in the previous study, to $N_d = 1 \times 10^{19}$ cm^{-3} for this study in an effort to further reduce the parasitic series resistance (R_s) of the devices.

The transfer-substrate process developed by the authors [4], [8] has been employed to transfer one quarter of a 2-in diameter InP-based epitaxial layer onto a 1-in^2 quartz wafer having a thickness of 70 μm. As the quartz wafer is thin, in order to reduce moding problems at high frequency operation, a support wafer is needed during the device processing. A 350-μm thick GaAs wafer has been employed, onto which the quartz wafer is

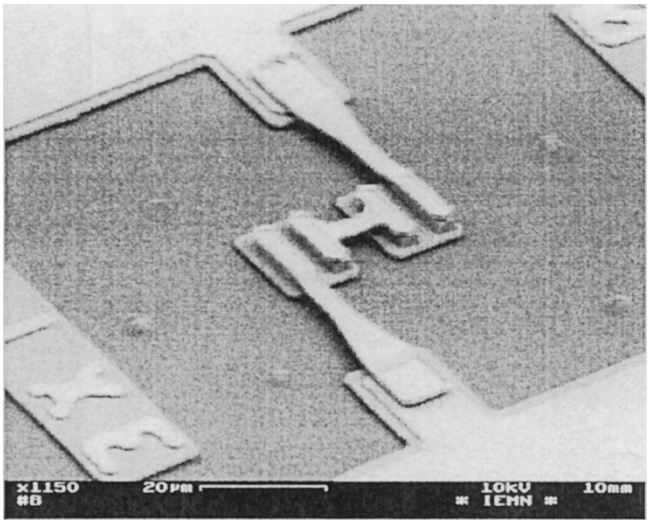

(a)

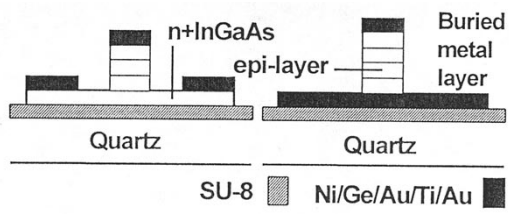

(b)

Fig. 1. (a) SEM micrograph of substrate-transferred air-bridge connected HBV diodes (3×16 μm) fabricated on 70 μm thick quartz. (b) Schematic diagrams of standard and buried metal layer (BML) configurations.

Manuscript received received July 10, 2000; revised September 13, 2000. This work was supported by the Centre Nationale d'Etudes Spatiales (CNES) and the European Space Agency (ESA), and was carried out within the framework of the Inter-European Terahertz Action (INTERACT) TMR program.

The authors are with the Institut d'Electronique et de Microélectronique du Nord (IEMN), UMR CNRS 8520, Université des Sciences et Technologies de Lille, 59652 Villeneuve d'Ascq Cedex, France (e-mail: Didier.Lippens@iemn.univ-lille1.fr).

Publisher Item Identifier S 1051-8207(00)10937-7.

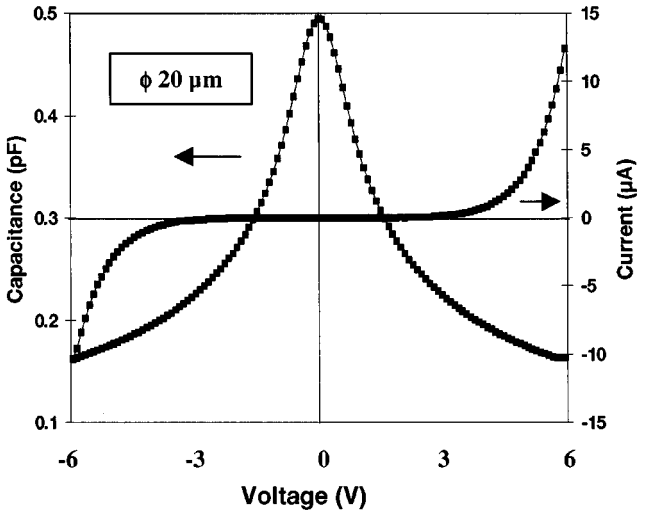

Fig. 2. $I-V$ (dc) and $(C-V)$ characteristics (4 GHz) for HBV diodes in coaxial configuration fabricated on 70 μm thick quartz.

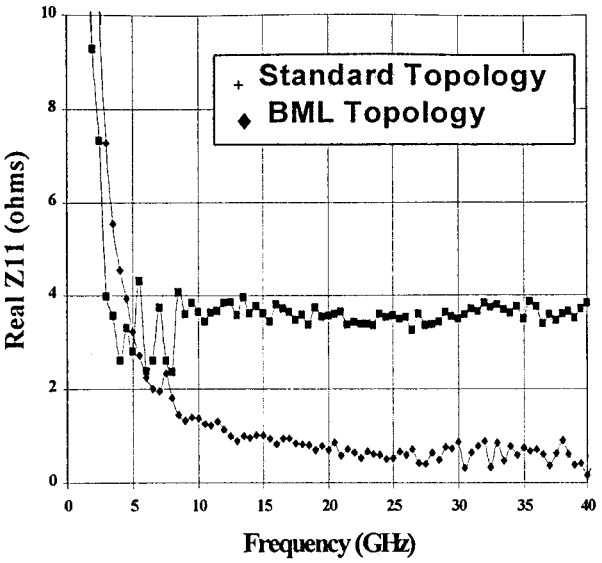

Fig. 3. Real part of Z_{11} for devices in coaxial configuration using the standard topology and the buried metal layer (BML) topology.

bonded into a pre-etched recess using a thin silicone-gel layer. In order to dissolve the InP substrate, an $HCl:H_2O$ (5 : 1) selective etch solution was used which has a high selectivity ratio between InGaAs and InP. After complete removal of the InP substrate, device processing was performed.

Three types of device configurations were incorporated into the mask-set for the measurements: coaxial type [active device area $(A) = 314\ \mu m^2$], air-bridge connected coplanar type ($A =$ 20–30 μm^2) and small area air-bridge contacted devices ($A =$ 12–96 μm^2). Fig. 1(a) shows a SEM micrograph of a typical HBV air-bridge connected device fabricated on quartz substrate using a combination of e-beam and photo-lithographic steps, the area of the mesa contact shown in Fig. 1(a) is 3 μm $\times$ 16 μm.

The air-bridged structures were fabricated using a set of nine masks. The primary ohmic contacts were formed using a sequential Ni/Ge/Au/Ti/Au metallization scheme and served as a self-aligned mask for the reactive ion etching (RIE) $(Ar:H_2:CH_4)$ of the mesas. A carefully controlled dry etch down to the n^+InGaAs layer was achieved in order to form the secondary ohmic contacts for all devices. The air-bridge structures were then fabricated using a bi-layer positive photo-resist process, further details of which can be found in [7].

The employment of a transfer-substrate process can enable the preservation a of vertical current flow via a new topological scheme, thus avoiding the so-called "spreading resistance" introduced by the planar current flow through the n^+InGaAs layer. Fig. 1(b) illustrates this by using two coaxial device configurations fabricated in this laboratory. The diode shown on the left-hand side has conventional planar side contacts. The configuration on the right hand side incorporates a buried metal layer (BML) which directly contacts the rear side of the mesa.

III. RF Measurements

Fig. 2 shows the current–voltage $(I-V)$ and capacitance–voltage $(C-V)$ characteristics for a substrate-transferred dual barrier HBV in coaxial configuration. In this case, the parasitic capacitance is negligible with respect to the intrinsic capacitance. As a consequence, the $(C-V)$ nonlinearity can be assessed without the necessity of de-embedding techniques. Some order of magnitude can also be evaluated for the series resistance in a coaxial type scheme. It can be seen that the devices display extremely symmetrical electrical characteristics. This demonstrates that we are able to preserve the high quality of the epitaxial layer during the substrate-transfer process. The devices exhibit excellent voltage handling, a leakage current as low as 3.8 A/cm^2 being observed at an applied voltage of 6 V. This demonstrates that the thicker AlAs layer is sufficient to prevent the leakage current degradation which results from the elevated doping, i.e., 2×10^{17} cm^{-3}, in the InGaAs cladding layers.

The $C-V$ characteristics for the transferred dual barrier HBV devices were measured at a frequency of 4 GHz. As with the $I-V$ characteristics, a highly symmetrical profile is observed, this is an essential characteristic for tripling and quintupling applications at high frequency since the output power in the odd-harmonics must be maximized. A zero-bias capacitance value of around 1.6 fF/μm^2 (i.e., 3.2 fF/μm^2 barrier) and a capacitance ratio of 3.4 : 1 were observed over the voltage range investigated. A slight degradation of this value compared to previous measurements can be explained by the increase in the doping level of the cladding layers. This very low capacitance level is a direct consequence of the epitaxial stacking of two diodes in series. These results are in very good agreement with calculations which we have made using a Poisson–Schrodinger equation solver.

Small-signal RF measurements were carried out on the basis of S- parameter measurements using a HP Vector Network Analyzer (VNA) over the frequency range 500 MHz to 110 GHz using three set-ups. For the RF measurements, the devices which had been fabricated in a coplanar-type (20–30 μm^2) and coaxial configuration were studied.

Let us first consider Fig. 3, which shows the frequency dependence (0.5–40 GHz) of the real part of the impedance mea-

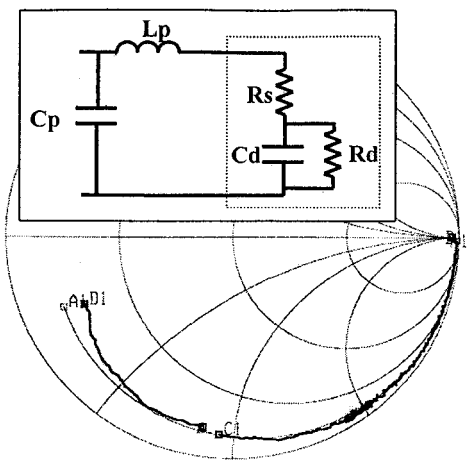

Fig. 4. Smith chart showing impedance locus for air-bridge connected coplanar configuration on 70-μm thick quartz (thick line-measured data, thin line-simulated data). Inset to figure shows the equivalent circuit for the device in coplanar configuration.

sured for the BML configuration in comparison with our previous measurements. After a rapid roll-off of Re(Z_{11}) due to the low value of parallel diode conductance (low leakage current) the value of Re(Z_{11}) becomes constant and fits the value of R_s. On this basis, a factor of 8 decrease is observed with R_s being 0.5 Ω for the present BML topology.

Turning now to the parasitic capacitance, we have plotted in Fig. 4 the locus of the S_{11} parameters measured between 0.5–110 GHz for an air-bridge connected configuration device in coplanar configuration (one mesa equivalent to two stacked barriers). De-embedding techniques are necessary in this case, and to this aim we have used a lumped element circuit given in the inset of Fig. 4. The various elements can be derived from a closer fit between the measurement via network analysis (HP ADS) taking into consideration the values of the intrinsic elements (C_d and R_d in Fig. 4) measured in coaxial configuration. In Fig. 4, C_p represents the parasitic capacitance. We have thus deduced the following values $C_p = 6$ fF, $L_p = 54$ pH, $R_s = 6$ Ω, $R_d \geq 10^4\Omega$, $C_d = 35$ fF at zero bias. An overall total parasitic capacitance of around 6 fF can be predicted, demonstrating a strong decrease of this term with respect to devices fabricated on thick semiconductor substrate. We have previously shown that the value of this capacitive parasitic is around 20 fF for devices in coplanar configuration fabricated on InP substrate. This reduction in capacitive parasitic can easily be explained by the difference in the value of the dielectric permittivity between InP and quartz.

This reduction in the value of the parasitic elements has two important consequences. Firstly, the cutoff frequency is dramatically increased via the reduction of the series resistance. For the present device, a cut-off frequency in the far infrared region can be predicted notably for multi-barrier devices whose capacitance is reduced according to the number of barriers (C_d/n). It should be noted that an increase in series resistance does not scale directly with n. Also, a decrease in the overall parasitic capacitance is of prime importance for small area devices for which large signal impedance matching can be troublesome. We are currently investigating the large-signal RF properties of the diodes. As a last comment, it must be noted that these small-signal measurements do not include the effects of velocity saturation of carriers which manifest under large-signal conditions [9], [10].

IV. Conclusion

In conclusion, important advances have been demonstrated on the basis of the transfer of InP-based HBV devices onto quartz which dramatically reduces the parasitic elements. It is believed that the present technology is quite generic and can be applied to other heterostructure barrier devices, notably the HBT's. In addition, the potential advantages of InP-based HBV diodes with respect to their GaAs counterparts are now established and permit one to envisage a Terahertz operation.

Acknowledgment

The authors would like to thank E. Delos for technical assistance during the small signal RF measurements.

References

[1] Q. Lee, S. C. Martin, D. Mensa, R. P. Smith, J. Guthrie, and M. J. W. Rodwell, "Submicron transferred-substrate heterojunction bipolar transistors," *IEEE Trans. Electron Device Lett.*, vol. 20, pp. 396–398, Aug. 1999.

[2] P. H. Siegel, R. P. Smith, M. C. Gaidis, and S. C. Martin, "2.5 THz GaAs monolithic membrane-diode mixer," *IEEE Trans. Microwave Theory Tech.*, vol. 47, pp. 596–604, May 1999.

[3] I. Mehdi, S. C. Martin, R. J. Dengler, R. P. Smith, and P. H. Siegel, "Fabrication and performance of planar Schottky diodes with T-Gate-like anodes in 200 GHz subharmonically pumped waveguide mixers," *IEEE Microwave Guided Wave Lett.*, vol. 6, pp. 49–51, Jan. 1996.

[4] S. Arscott, P. Mounaix, and D. Lippens, "Transferred InP-based HBV's on glass substrate," *Electron. Lett.*, vol. 35, pp. 1493–1494, Aug. 1999.

[5] E. L. Kollberg and A. Rydberg, "Quantum-barrier-varactor diode for high efficiency millimeter-wave multiplier," *Electron. Lett.*, vol. 25, pp. 1696–1697, 1989.

[6] X. Mélique, A. Maestrini, M. Faureau, O. Vanbésien, J. M. Goutoule, G. Beaudin, T. Nahri, and D. Lippens, "Record performance of a 250 GHz InP-based heterostructure barrier varactor tripler," *Electron. Lett.*, vol. 35, pp. 938–939, May 1999.

[7] X. Mélique, A. Maestrini, E. Lheurette, P. Mounaix, M. Faureau, O. Vanbésien, J. M. Goutoule, G. Beaudin, T. Nähri, and D. Lippens, "12% efficiency and 9.5 dBm output power from InP-based heterostructure barrier varactor triplers at 250 GHz," in *IEEE MTT Symp.*, Anaheim, CA, USA, June 1999.

[8] S. Arscott, P. Mounaix, and D. Lippens, "Substrate transfer process for InP-based heterostructure barrier varactor devices," *J. Vac. Sci. Technol. B*, vol. 18, pp. 150–155, Jan. 2000.

[9] B. B. Van Iperen and H. Tjassens, "Influence of carrier velocity saturation in the unswept layer on the efficiency of avalanche transit time diodes," *Proc. IEEE*, vol. 59, p. 1032, June 1971.

[10] E. Kolberg, T. J. Tolmunen, M. A. Frerking, and J. R. East, "Current saturation in submillimeter-wave varactors," *IEEE Trans. Microwave Theory Tech.*, vol. 40, p. 831, May 1992.